Research Article | Vol. 26, No. 13 | 25 Jun 2018 | OPTICS EXPRESS 16624
Optics EXPRESS

Mapping the dynamical regimes of a SESAM mode-locked VECSEL with a long cavity using time series analysis

TUSHAR MALICA,[1,4] JIPENG LIN,[2] THORSTEN ACKEMANN,[3] DOUGLAS J. LITTLE,[1] JOSHUA P. TOOMEY,[1] DAVID PABŒUF,[2] WALTER LUBEIGT,[2] NILS HEMPLER,[2] GRAEME MALCOLM,[2] GARETH T. MAKER,[2] AND DEBORAH M. KANE[1,5]

[1]*Photonics Dynamical Systems Group, Department of Physics & Astronomy, Macquarie University, Sydney 2109, Australia*
[2]*M-Squared Ltd, 1 Kelvin Campus, West of Scotland Science Park, Glasgow G4 0NG, Scotland, UK*
[3]*Deaprtment of Physics, University of Strathclyde, John Anderson Building, Glasgow G4 0NG, Scotland, UK*
[4]*tushar.malica@mq.edu.au*
[5]*deb.kane@mq.edu.au*

Abstract: The different dynamical regions of an optically-pumped SESAM mode-locked, long-cavity VECSEL system with a fundamental pulse repetition frequency of ~200 MHz are investigated. The output power, captured as 250 μs long time series using a sampling rate of 200 GSa/s, for each operating condition of the system, is analyzed to determine the dynamical state. A wavelength range of 985-995 nm and optical pump powers of 10 W-16.3 W is studied. The system produces high quality fundamental passive mode-locking (FML) over an extensive part of the parameter space, but the different dynamical regions outside of FML are the primary focus of this study. We report five types of output: CW emission, FML, mode-locking of a few modes, double pulsing, and, semi-stable 4th harmonic mode-locking. The high sampling rate of the oscilloscope, combined with the long duration of the time series analyzed, enables insight into how the structure and substructure of pulses vary systematically over thousands of round trips of the laser cavity. Higher average output power is obtained in regions characterized by semi-stable 4th harmonic mode-locking than observed for FML, raising whether such average powers might be achieved for FML. The observed dynamical transitions from fundamental mode-locking provide insights into instability challenges in developing a stable, widely tunable, low repetition rate, turn-key system; and to inform future modelling of the system.

OCIS codes: (140.3460) Lasers; (140.4050) Mode-locked lasers; (140.5960) Semiconductor lasers; (140.7090) Ultrafast lasers; (140.7260) Vertical cavity surface emitting lasers.

References and links

1. C. R. Head, B. Bialkowski, J. Lin, W. Lubeigt, N. Hempler, G. T. Maker, and G. P. A. Malcolm, "Commercial Mode-Locked Vertical-External-Cavity Surface-Emitting Lasers," in 2017 European Conference on Lasers and Electro-Optics and European Quantum Electronics Conference, (Optical Society of America, 2017), paper CB_8_2.
2. W. Lubeigt, B. Bialkowski, J. Lin, C. Robin Head, N. Hempler, G. T. Maker, and G. P. A. Malcolm, "Commercial mode-locked vertical external cavity surface emitting lasers," Proc. SPIE **10087**, 100870D (2017).
3. L. Kornaszewski, N. Hempler, C. J. Hamilton, G. T. Maker, and G. P. A. Malcolm, "Advances in mode-locked semiconductor disk lasers," Proc. SPIE **8606**, 86060N (2013).
4. N. Hempler, W. Lubeigt, B. Bialkowski, C. J. Hamilton, G. T. Maker, and G. P. A. Malcolm, "Advances in commercial, mode-locked vertical external cavity surface emitting lasers," Proc. SPIE **9734**, 97340X (2016).
5. N. Hempler, B. Bialkowski, C. J. Hamilton, G. T. Maker, and G. P. A. Malcolm, "Development and commercialization of mode-locked VECSELs," Proc. SPIE **9349**, 93490K (2015).

#326005 https://doi.org/10.1364/OE.26.016624
Journal © 2018 Received 16 Mar 2018; revised 7 Jun 2018; accepted 7 Jun 2018; published 14 Jun 2018

Optics EXPRESS

6. R. Paschotta, R. Häring, A. Garnache, S. Hoogland, A. C. Tropper, and U. Keller, "Soliton-like pulse-shaping mechanism in passively mode-locked surface-emitting semiconductor lasers," Appl. Phys. B **75**(4–5), 445–451 (2002).
7. C. G. E. Alfieri, D. Waldburger, S. M. Link, E. Gini, M. Golling, G. Eisenstein, and U. Keller, "Optical efficiency and gain dynamics of modelocked semiconductor disk lasers," Opt. Express **25**(6), 6402–6420 (2017).
8. E. J. Saarinen, A. Härkönen, R. Herda, S. Suomalainen, L. Orsila, T. Hakulinen, M. Guina, and O. G. Okhotnikov, "Harmonically mode-locked VECSELs for multi-GHz pulse train generation," Opt. Express **15**(3), 955–964 (2007).
9. J. E. Ehrlich, D. T. Neilson, A. C. Walker, G. T. Kennedy, R. S. Grant, W. Sibbett, and M. Hopkinson, "Carrier lifetimes in MBE and MOCVD InGaAs quantum wells," Semicond. Sci. Technol. **8**(2), 307–309 (1993).
10. Y. C. Chen, P. Wang, J. J. Coleman, D. P. Bour, K. K. Lee, and R. G. Waters, "Carrier recombination rates in strained-layer InGaAs-GaAs quantum wells," IEEE J. Quantum Electron. **27**(6), 1451–1455 (1991).
11. C. Baker, M. Scheller, S. W. Koch, A. R. Perez, W. Stolz, R. J. Jones, and J. V. Moloney, "In situ probing of mode-locked vertical-external-cavity-surface-emitting lasers," Opt. Lett. **40**(23), 5459–5462 (2015).
12. J. Hader, M. Scheller, A. Laurain, I. Kilen, C. Baker, J. V. Moloney, and S. W. Koch, "Ultrafast non-equilibrium carrier dynamics in semiconductor laser mode-locking," Semicond. Sci. Technol. **32**(1), 013002 (2017).
13. C. A. Zaugg, M. Hoffmann, W. P. Pallmann, V. J. Wittwer, O. D. Sieber, M. Mangold, M. Golling, K. J. Weingarten, B. W. Tilma, T. Südmeyer, and U. Keller, "Low repetition rate SESAM modelocked VECSEL using an extendable active multipass-cavity approach," Opt. Express **20**(25), 27915–27921 (2012).
14. M. A. Gaafar, A. Rahimi-Iman, K. A. Fedorova, W. Stolz, E. U. Rafailov, and M. Koch, "Mode-locked semiconductor disk lasers," Adv. Opt. Photonics **8**(3), 370–400 (2016).
15. B. W. Tilma, M. Mangold, C. A. Zaugg, S. M. Link, D. Waldburger, A. Klenner, A. S. Mayer, E. Gini, M. Golling, and U. Keller, "Recent advances in ultrafast semiconductor disk lasers," Light Sci. Appl. **4**(7), e310 (2015).
16. U. Keller, "Recent developments in compact ultrafast lasers," Nature **424**(6950), 831–838 (2003).
17. M. Guina, A. Rantamäki, and A. Härkönen, "Optically pumped VECSELs: review of technology and progress," J. Phys. D Appl. Phys. **50**(38), 383001 (2017).
18. F. F. Voigt, F. Emaury, P. Bethge, D. Waldburger, S. M. Link, S. Carta, A. van der Bourg, F. Helmchen, and U. Keller, "Multiphoton in vivo imaging with a femtosecond semiconductor disk laser," Biomed. Opt. Express **8**(7), 3213–3231 (2017).
19. R. Aviles-Espinosa, G. Filippidis, C. Hamilton, G. Malcolm, K. J. Weingarten, T. Südmeyer, Y. Barbarin, U. Keller, S. I. C. O. Santos, D. Artigas, and P. Loza-Alvarez, "Compact ultrafast semiconductor disk laser: targeting GFP based nonlinear applications in living organisms," Biomed. Opt. Express **2**(4), 739–747 (2011).
20. P. G. Antal and R. Szipőcs, "Tunable, low-repetition-rate, cost-efficient femtosecond Ti:sapphire laser for nonlinear microscopy," Appl. Phys. B **107**(1), 17–22 (2012).
21. O. E. Martinez, "Grating and prism compressors in the case of finite beam size," J. Opt. Soc. Am. B **3**(7), 929–934 (1986).
22. E. B. Treacy, "Compression of picosecond light pulses," Phys. Lett. A **28**(1), 34–35 (1968).
23. E. Treacy, "Optical pulse compression with diffraction gratings," IEEE J. Quantum Electron. **5**(9), 454–458 (1969).
24. S. Sugavanam, N. Tarasov, and D. V. Churkin, "Real-Time Intensity Domain Characterization of Fibre Lasers Using Spatio-Temporal Dynamics," Appl. Sci. **6**(3), 65 (2016).
25. F. Gustave, N. Radwell, C. McIntyre, J. P. Toomey, D. M. Kane, S. Barland, W. J. Firth, G.-L. Oppo, and T. Ackemann, "Observation of Mode-Locked Spatial Laser Solitons," Phys. Rev. Lett. **118**(4), 044102 (2017).
26. W.-W. Hsiang, C.-Y. Lin, N. Sooi, and Y. Lai, "Long-term stabilization of a 10 GHz 0.8 ps asynchronously mode-locked Er-fiber soliton laser by deviation-frequency locking," Opt. Express **14**(5), 1822–1828 (2006).
27. A. Khadour, S. Bouchoule, G. Aubin, J. C. Harmand, J. Decobert, and J. L. Oudar, "Ultrashort pulse generation from 1.56 μm mode-locked VECSEL at room temperature," Opt. Express **18**(19), 19902–19913 (2010).
28. S. Longhi, P. Laporta, S. Taccheo, and O. Svelto, "Third-order-harmonic mode locking of a bulk erbium:ytterbium:glass laser at a 2.5-GHz repetition rate," Opt. Lett. **19**(23), 1985–1987 (1994).
29. I. Kilen, J. Hader, J. V. Moloney, and S. W. Koch, "Ultrafast nonequilibrium carrier dynamics in semiconductor laser mode locking," Optica **1**(4), 192–197 (2014).
30. A. Mysyrowicz, D. Hulin, A. Antonetti, A. Migus, W. T. Masselink, and H. Morkoç, "Dressed Excitons' in a Multiple-Quantum-Well Structure: Evidence for an Optical Stark Effect with Femtosecond Response Time," Phys. Rev. Lett. **56**(25), 2748–2751 (1986).
31. A. Von Lehmen, D. S. Chemla, J. E. Zucker, and J. P. Heritage, "Optical Stark effect on excitons in GaAs quantum wells," Opt. Lett. **11**(10), 609–611 (1986).
32. S. Tsuda, W. H. Knox, S. T. Cundiff, W. Y. Jan, and J. E. Cunningham, "Mode-locking ultrafast solid-state lasers with saturable Bragg reflectors," IEEE J. Sel. Top. Quantum Electron. **2**(3), 454–464 (1996).
33. U. Keller and A. C. Tropper, "Passively modelocked surface-emitting semiconductor lasers," Phys. Rep. **429**(2), 67–120 (2006).
34. O. Sieber, M. Hoffmann, V. Wittwer, M. Mangold, M. Golling, B. Tilma, T. Sudmeyer, and U. Keller, "Experimentally verified pulse formation model for high-power femtosecond VECSELs," Appl. Phys. B **113**(1), 133–145 (2013).

Optics EXPRESS

35. M. Hoffmann, O. D. Sieber, D. J. H. C. Maas, V. J. Wittwer, M. Golling, T. Südmeyer, and U. Keller, "Experimental verification of soliton-like pulse-shaping mechanisms in passively mode-locked VECSELs," Opt. Express **18**(10), 10143–10153 (2010).

1. Introduction

Long-cavity vertical external cavity surface emitting lasers (VECSELs), or, semiconductor disk lasers (SDLs) with pulse repetition frequency (PRF) of the order of 100-200 MHz are being used as a first-stage pre-compression unit in cost-effective laser systems for applications such as nonlinear microscopy. They can augment, or potentially replace TiSa based laser systems [1–5]. Passive mode-locking is usually achieved via a semiconductor saturable absorber mirror (SESAM). Strong gain saturation at high pump powers has been a limitation to the potential for SESAM-VECSEL systems to attain robust, fundamental passive mode-locking (FML) in the few hundred MHz pulse repetition frequency region with high power efficiency. As a result, long-cavity VECSELs can be limited to operate near laser threshold, where gain saturation is weaker, to achieve FML [6,7]. Earlier works have shown a direct relation between increased pump power and the onset of harmonic mode-locking (HML), with the order of the harmonic having been observed to increase linearly with optical pump power [8]. In this contribution, we explore the different dynamical regimes observed in an optically pumped SESAM-VECSEL with a low PRF of ~200 MHz for FML in the time domain with simultaneous high sampling rate and large storage capacity.

The lower limit of achievable repetition rate and associated power scalability in SESAM mode-locked VECSEL systems, to-date, has been limited due to a short upper state carrier lifetime in the semiconductor gain material, calculated to be typically a few nanoseconds [7,9]. It is found to be structure-dependent rather than being an intrinsic material property [10]. The carrier lifetime should ideally be larger than the inter-pulse period of the FML pulse so that all energy from the excited carriers in the conduction band may contribute to pulse amplification. For a low PRF VECSEL, the interaction time between the incoming pulse and the excited carriers in the semiconductor gain chip is shorter than the cavity round-trip time. The excited carriers contribute to spontaneous recombination in the time between the pulses and decrease the differential efficiency [7]. The semiconductor gain material, therefore, is intrinsically more suitable for higher repetition rate systems and destabilization of FML becomes more probable in low PRF VECSELs. Additionally, it has been proven that most gain recovery occurs within a few picoseconds [11]. A recovery time faster than the cavity round-trip time of a few nanoseconds in the case of low PRF, favours splitting of the gain, resulting in multiple pulses circulating inside the laser cavity [8]. Also, carrier-centric processes, including spontaneous recombination and Auger recombination, heavily affect mode-locking and have been shown to have lifetimes ranging from a few hundred picoseconds to a few nanoseconds [12]. These processes are not constant over the cavity round-trip time of a long-cavity VECSEL. Combining this with the need to balance intracavity dispersion, it is a significant design challenge to maintain the entire gain in a single, fundamental pulse in a long cavity VECSEL system.

From the perspective of cavity design, the relative location of the VCSEL gain chip and SESAM within the external cavity is of great importance. Previous research has found that a folded-cavity configuration with the gain chip placed at the geometric center of the cavity is a good compromise for minimizing multi-pulsing per round-trip behavior, or non-FML output [2]. This results in equidistant consecutive pulses with minimum discrepancy in inter-pulse period while achieving a minimal increase in geometric complexity of the laser layout.

All of these challenges have contributed to there being few successful commercially available VECSEL systems at low PRF to date [13,14]. In contrast, the development of systems in the GHz PRF range has been quite intense in the last decade [14–17]. An increased commercial demand for low PRF systems in fields like biomedical photonics, chemistry, and, nonlinear microscopy in the recent years has certainly fuelled interest within the laser research community [18,19]. Achieving turn-key systems with low repetition rates combined

Optics EXPRESS

with high peak and average output power, wide-tunability and short pulse duration, will support such systems to become an alternative to the conventionally used Ti:Sa laser technologies operating at a PRF as low as 80 MHz [20] in these fields. Also, VECSELs are known to have a better cost to wavelength flexibility figure of merit compared to the Ti:Sa lasers currently used. In order to be able to address the stated challenges, knowledge of the dynamics outside the FML regime is needed. In turn, this will allow due consideration of how these transitions might be suppressed in favour of an extended range of FML output. This study explores the evolution from FML operation to other dynamics using conventionally optimised system conditions.

This paper is organized as follows. Section 2 describes the experimental setup used for data acquisition. Section 3 reports four dynamical regions, in addition to FML, as we steer the system outside the range of optimum operating conditions for FML. Two of these regions have a sub-region where the low-frequency variation of otherwise stable pulses is observed. The observed dynamical transitions from fundamental mode-locking give insights into factors contributing to mode-locking instabilities and complexity in long cavity VECSELs. The acquired data shows availability of an even higher amount of gain which is not being accessed in the FML region currently. This may open up the possibility of both extending the range of operating conditions exhibiting FML, and of obtaining increased average power in the FML region. A state-of-the-art oscilloscope with a bandwidth of 30 GHz and a sampling rate of 200 GS/s is used to capture 250 μs long time series at each operating condition, defined by, wavelength and pump laser diode current. We exploit the capabilities of this modern oscilloscope to capture each time series with 50×10^6 data points at 5 ps sampling time. This is a much longer total time, nearly 5×10^4 round-trips for this long-cavity VECSEL, than has been previously analyzed in studies of mode-locked laser system dynamics. It allows systematic variations in the laser dynamics on longer time scales to be investigated, including relatively rare events. The pulses are relatively long with a duration of a few tens of picoseconds. Under these conditions, the high sampling rate allows some, though not all, details of the pulses to be resolved. The pulse duration may be shortened further to ultrafast or femtosecond scale, using pulse compression techniques based on diffraction gratings [4,21–23]. Finally, we conclude our observations in section 4. This paper reports the observed dynamics in a SESAM mode-locked, long-cavity VECSEL system, acquired using the state-of-the-art diagnostic system, to provide results that may enable the research community to resolve instability issues encountered in the system, in the future.

2. Experiment

The laser system layout used to achieve a pulse repetition frequency (PRF) of ~200 MHz is shown in Fig. 1. It is a folded-cavity VECSEL system with the semiconductor gain chip placed in the geometric center of the cavity. The semiconductor gain chip is a typical monolithic VCSEL structure with the laser-cavity-facing end mirror omitted in favor of a capping and confinement layer through which pump light enters and light emission exits. The active region has multiple quantum wells sandwiched between pump absorbing layers (InGaAs-based). This sandwich is grown on a distributed Bragg reflector (DBR) which in-turn was grown on a GaAs substrate. The whole structure is mounted on a copper plate. This semiconductor gain chip was designed to operate with optical pump power ranging between 9.5 - 31.7 W, corresponding to diode laser currents of 17 - 40 A, and with the central peak of the gain at a wavelength of 990 nm. The optical– pump is an 808 nm laser diode with a pump spot diameter of 200 μm. The angle between the pump laser diode and semiconductor gain chip was kept as small as possible to ensure a better mode matching between pump diode and cavity mode. A single-crystal synthetic diamond, having a 2° wedge to avoid Febry-Perot effects, served as a heat spreader and was bonded to the semiconductor gain, while the unbonded opposite surface was coated with an anti-reflection coating of less than 1% reflectivity for 920-1050 nm.

Optics EXPRESS

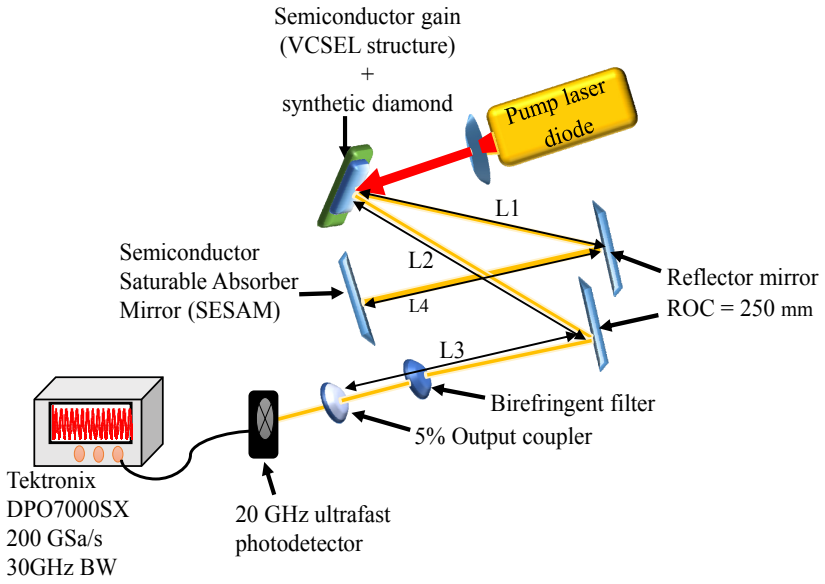

Fig. 1. Experimental setup for passive mode-locking using an optically pumped VCSEL semiconductor gain and SESAM with a pulse repetition rate of ~200 MHz with cavity round-trip length ~1.5 m. ROC- radius of curvature. BW – bandwidth.

A single quantum well SESAM was maintained at 23°C, using a thermoelectric cooler (TEC), throughout the experiment. It was grown using the same substrate and DBR material as the semiconductor gain chip. A single plate birefringent filter placed at Brewster's angle within the cavity, allowed manual tuning of the VECSEL wavelength. The output power was measured with a 20 GHz ultrafast-20MM photodetector (Advanced Laser Diode Systems) connected to a Tektronix DPO7000SX oscilloscope using 200 GSa/s sampling rate. The discretized output time series obtained from the oscilloscope were saved as a 250 μs long time series corresponding to 50×10^6 data points collected at 5 ps intervals. The output power time series were collected at pump laser diode currents ranging from 24 A to 18 A at intervals of 1 A. The linear relationship between the laser diode pump power and diode current is observed to follow the equation, $y = 0.9685x - 6.9326$, with x as the pump laser diode current (A) and y is the pump power (W). 18 A corresponds to ~10.5 W and 24 A to ~16.3 W. At each laser diode pump source current value, a systematic VECSEL wavelength scan, from the highest lasing wavelength to the lowest wavelength, in 1nm decrements, was completed.

3. Results and description of the dynamical regimes

Figure 2 shows the measured average output power as a function of VECSEL output wavelength and pump laser diode current. Operating points bounded in colored ellipses were found to have an almost linear relationship between average output power and the pump laser diode current at the respective wavelength value. The low-power region, with average output power less than 0.16 W, displayed a CW signal with low amplitude noise and with no observed pulsing. The medium average power region displayed average output power greater than 0.22 W but lower than 0.95 W. Lastly, operating conditions with average output power greater than 1 W were designated as the high average power region. The rich variety of dynamical transitions, away from FML, are observed at the operating conditions lying in the high-power region, and operating points close to this region in the medium-power region, at shorter lasing wavelengths having pump laser diode currents upwards of 20 A.

Optics EXPRESS

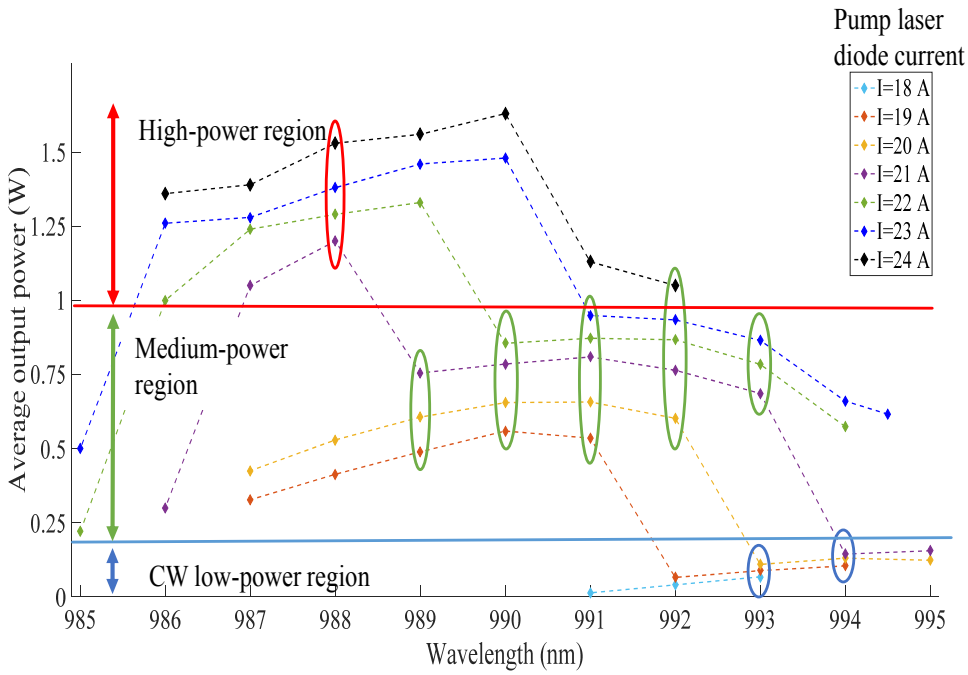

Fig. 2. The average output power (W) for each pump laser diode current (18 A - 24 A) is plotted as a function of VECSEL output wavelength (nm) and classified into three regions (i) CW low power region < 0.16 W, (ii) Medium power region between 0.22 W and 0.95 W, and (iii) high-power region >1 W. Points enclosed within ellipses indicate wavelengths at which the average output power has an almost linear relationship to the pump laser diode current.

Figure 3 shows dynamical behavior observed at each operating condition over the complete parameter space. Each condition, defined by the VECSEL output wavelength and pump laser diode current, is represented with a colored circle, where the color, as calibrated by the color bar located on the right, indicates the average output power as seen in Fig. 2. Fundamental passive mode-locking (FML) with a characteristic single pulse circulating inside the laser cavity is found to be the dominant dynamics within the range of operation in the parameter space. This is shown by the large green-line-bounded region in Fig. 3. The peak of the output power was experimentally observed at wavelengths ranging between 990 nm-992 nm for FML with a longer wavelength found at higher pump laser diode current (pump power).

Four additional dynamical regions and two low-frequency modulation effected destabilized sub-regions are observed away from the peak of the gain and the boundaries of these regions are shown in Fig. 3. Dynamical transition to multi-pulsing is observed at shorter wavelengths and higher pump laser diode currents. CW operation is observed outside the FML region at longer wavelengths. At one operating condition, stable double-pulsing is observed. Several operating conditions give semi-stable pulsing which is shown to be consistent with semi-stable fourth order harmonic mode-locking. This region has high average power. Two destabilized locking sub-regions were observed which exhibited either double or single pulsing per round-trip and which show systematic pulse splitting and restabilization occurring over a few hundred round-trips. Lastly, a region of mode-locking of a small number of modes is seen which also has unexpectedly high average output power. Each type of observed output is described in more detail below.

Optics EXPRESS

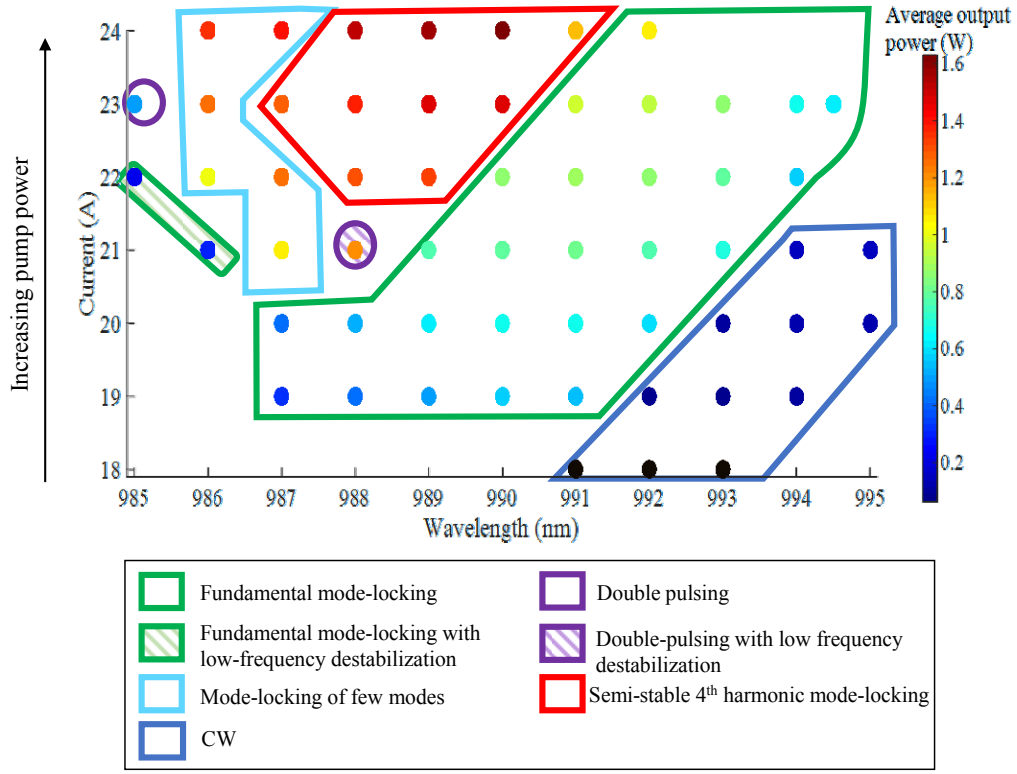

Fig. 3. Dynamical classification of the parameter space region. Each operating condition, defined by a manually tuned wavelength value and pump source drive current is represented with a colored circle, where, the color indicates the average output power as seen in Fig. 2 and calibrated by the color bar on the right of the figure.

3.1 Fundamental passive mode-locking (FML)

The region displaying FML is observed at operating conditions bounded by the green perimeter (both hatched and plain regions) as seen in Fig. 3. The 250 μs long time series were found to contain 49,037 ± 1 pulses for stable FML cases bounded by the green line and without hatching. The average inter-pulse period ~5.0981 ns (found to be constant to a 4 decimal place precision for FML operating points) corresponds to the round-trip for the laser cavity as observed from the first peak in the RF power spectrum (196.152 MHz), obtained using a fast Fourier transform of the time series. This peak was ~70 dB above the noise floor. The standard deviation of the inter-pulse period for operating conditions lying within this region was found to have a value between 5 ps and 12 ps depending on the parameters. 5 ps is the sampling period.

Figure 4 shows a space-time representation of the single pulse within each round-trip, for 100 round-trips [24,25]. Each pixel in the figure is a representation of the acquired discrete signal amplitude for one sampling period of the oscilloscope and is scaled to the color according to the color-scale located on the right hand side of the figure. The horizontal axis represents the time interval within a single laser cavity round-trip, scaled between 0 and 1, where, 1 indicates the average inter-pulse period of 5.0981 ns or ~1020 sampling periods. This single round-trip temporal axis represents the spatial domain of the cavity. Due to the average round-trip time being a non-integer multiple of the sampling time and limited precision of the computed average value, an optimization of the visual appearance using pixel correction is introduced in each space-time representation presented here onwards. The vertical axis represents the number of the round-trip. This axis is interpreted as the temporal

Optics EXPRESS

domain and shows the position of the laser pulse within the cavity over time. Much care was taken to optimize the correction while maintaining the resolution of the pulses. Each space-time representation was corrected by inserting a pixel equivalent to zero signal amplitude in the beginning of every third round trip and the remaining 1019 data points are extracted from the captured data. It should be noted that an additional pixel correction is needed when viewing thousands of round-trips as the slightest of pixel non-alignment compounds. This is clearly stated wherever applied to space-time representations presented in the following sections. For the purpose of the results presented in this paper, the correctional pixel always represents a zero signal amplitude and is introduced as the first data point of the specified round-trip.

The spatial position of the pulse inside the laser cavity as shown in Fig. 4 is constant with increasing round-trip count. This occurs over all, nearly 5×10^4, round-trips. The FML pulse durations were observed to have values between 23 ± 5 ps and 56 ± 20 ps for the different FML operating conditions within the main green-line bounded region of Fig. 3. This paper gives an overview of the dynamical regimes observed in this long-cavity VECSEL. A description of FML pulsing behavior and ways to quantify pulse quality is outside the scope of this paper and will be presented elsewhere.

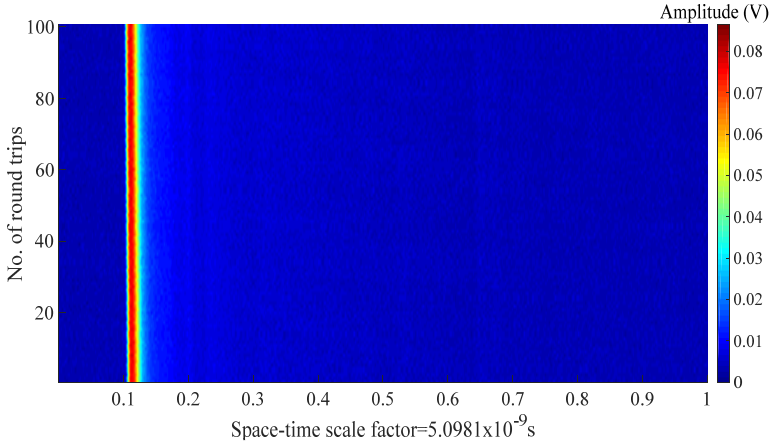

Fig. 4. 0.5 μs subset of the time series captured at 991 nm and 23 A, displayed in a space-time representation showing a single pulse over 100 round-trips. The horizontal axis represents the laser cavity roundtrip consisting of ~1020 consecutive data points captured at 5ps sampling time. One round-trip is 5.0981 ns. The vertical axis represents consecutive round-trip times captured by the oscilloscope and stacked one above the other to show the pulse evolvement over time.

3.1.1 Fundamental passive mode-locking with low frequency destabilization

A region in which fundamental passive mode-locking is destabilized by a low frequency envelope is present in the green-line-bounded, striped region in Fig. 3. Operating conditions lying in this region show single-pulsed, mode-locked output similar to the FML region, but, also displaying smaller windows of time with increased pulse-height variation lasting a few hundred round-trips which occur every ~3269th round-trip for the VECSEL tuned to 986 nm and 21 A. Changes in pulse duration and inter-pulse period accompany the pulse height variation. The space-time dynamics during this time can be seen in Fig. 5(a) with additional pixel correction as described in section 3.1. The pulse remains in the same spatial position within the cavity but its sub-structure goes through a systematic variation involving the appearance of subsidiary peaks within the pulse envelope which then revert to the single pulse envelope after about 300 round trips. The first sub-peak is mostly observed to be ~35 ps - 45 ps [Fig. 5(b)] away from the peak amplitude of the pulse. The second sub-peak is ~58 ps-70 ps [Fig. 5(b)] away. These pulse-peak-to-sub-peak period ranges have normal distribution.

Optics EXPRESS

During the window of mode-locking destabilization [Fig. 5(a)], the leading edge of the pulse maintains stability and spatial position, while, the trailing edge systematically experiences changes in the envelope structure with initial pulse-peak-to-sub-peak period being of higher value. As the time elapses and higher round-trips within the destabilization window are reached, the sub-peaks gradually shift towards the pulse-peak. Sub-peaks closer to the pulse-peak have higher amplitude with cases where peaks of the previously observed two sub-peaks are almost at the same amplitude as seen in Fig. 5(c). Eventually, the pulse structure, devoid of any sub-peaks, is restored as the system exits the window of destabilization. Figure 5(d) shows a pulse close to the restoration of the typical pulse just before the system exits from the destabilization window. This phenomenon has consequences in the frequency domain as well.

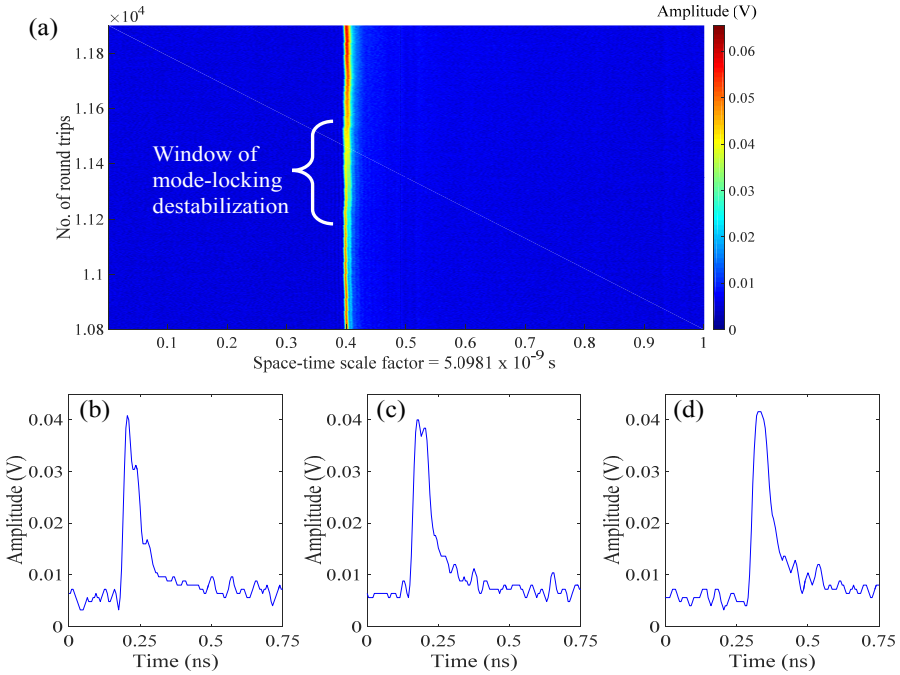

Fig. 5. (a) A space-time plot, obtained at 986 nm and 21 A, showing a window of time displaying transient locking with additional pixel correction. Sample pulses captured at progressive round-trips are shown in (b)-(d): (b) prominent pulse sub peaks at 11300th round-trip, (c) 11430th round-trip, and, (d) 11490th round-trip.

The RF spectrum for the time series shows two sidebands on each side of the cavity resonance peak at ~60 kHz and ~120 kHz from the resonance peak. The 60 kHz frequency corresponds to the frequency at which destabilization and initiation of the pulse sub-structure sequence - occurs. The RF spectrum of a subset of the time series which does not include the window of mode-locking destabilization is observed to have the typical RF spectrum as seen for stable FML. Low modulation frequencies similar to the one observed here have been previously observed in asynchronous mode-locked fiber lasers [26]. It is important to note that stable mode-locking for extended periods of time can be interrupted by short periods of destabilization. The other operating point showing this behavior occurs at 985 nm and 22 A. It is closer to stable FML with only one fully-developed sideband on either side of the cavity resonance frequency peak spaced by ~30 kHz.

3.2 Double pulsing

One operating point in the parameter space (985 nm, 23 A), indicated by the purple-line encircled point in Fig. 3, exhibited stable double-pulsing behavior. This point has low average

Optics EXPRESS

output power ~0.5 W and low peak amplitudes for the pulses. Figure 6(a) shows the space-time plot at this operating point for 100 round-trips. The temporal position of the two pulses inside the laser cavity is unchanged over time. The time trace for ~2 round-trips is shown in Fig. 6(b). The average inter-pulse durations are (~1.284 ± 0.007) ns followed by (~3.814 ± 0.007) ns which repeat throughout the time series. The inter-pulse separations correspond to one quarter and three quarters of the round-trip time so this mode of operation is consistent with 4th harmonic mode-locking with two pulses missing in the sequence.

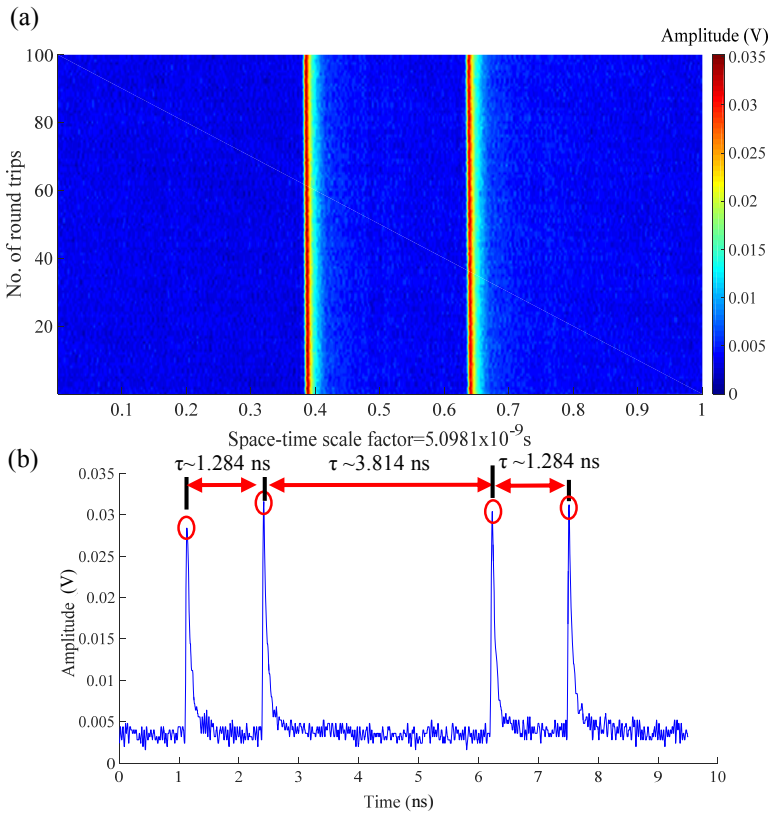

Fig. 6. (a) Space-time plot for a 0.5μs subset of the time series captured at 985 nm, 23 A; (b) average inter-pulse durations shown for a sample of pulse train.

3.2.1 Double-pulsing with low frequency destabilization

An operating point at which double-pulsing is destabilized by a low frequency envelope is present at 988 nm and 21 A. The point with this dynamical signature is encircled and striped in purple in Fig. 3. It shows time windows of pulse destabilization, manifesting as a systematic sequence of pulse broadening and evolving sub-structure shown in Fig. 7(a). Additional pixel correction was necessary in generating this space-time plot which extends over 5000 round trips to take account of the round trip being a non-integer number of round trips. The pulses then stay in nominally the same relative positions within the laser cavity over all the round-trips. The broadening of the pulse and evident sub-structure is observed to be triggered at the leading edge of the first pulse, followed by a systematic decrease of the pulse peak amplitude of this pulse. The first pulse then restabilizes before the second pulse in the cavity is observed to follow a similar pattern of destabilization and restabilization, after which the system returns to two clean pulses. Figures 7(b) and 7(c) show samples of the pulse profiles of the destabilized pulses observed in this region. The destabilization of mode-locking and pulse sub-structure changes are similar to observations made in section 3.1 but

Optics EXPRESS

with a modulation frequency of ~40 kHz and a second harmonic observed at ~80 kHz. The average inter-pulse durations between the two pulses are (~3.82 ± 0.06) ns and (~1.28 ± 0.06) ns. That is, similar to the stable double pulsed operation.

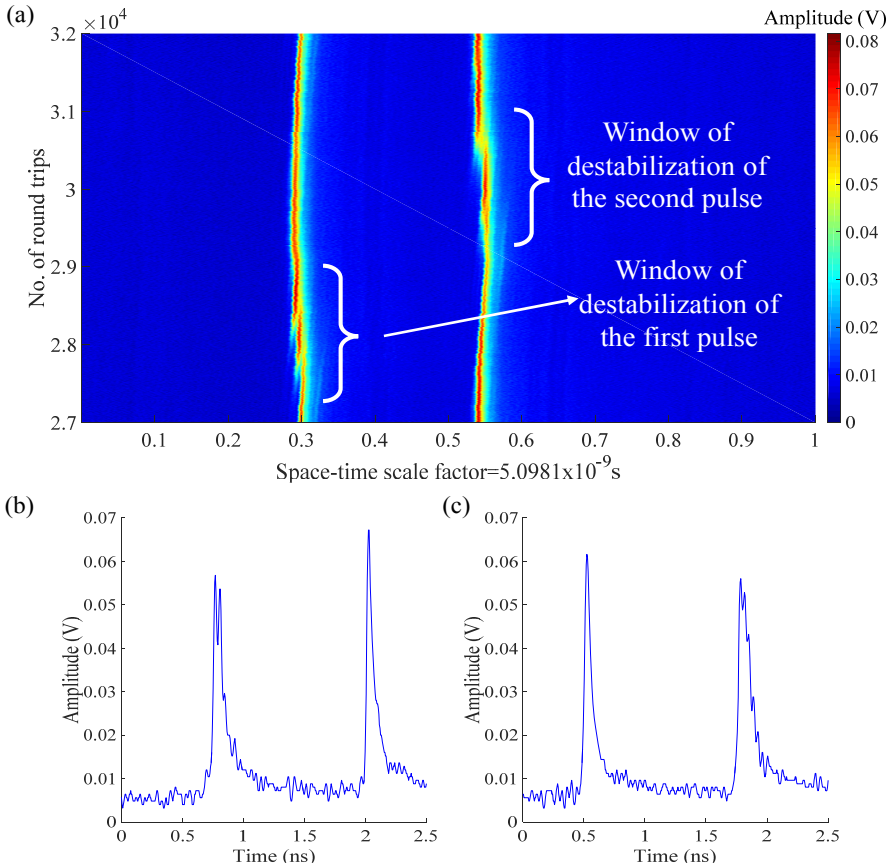

Fig. 7. (a) Space-time plot of 5000 round-trips showing window of destabilization of the first pulse followed by a window of destabilization of the second pulse with increasing number of round-trips. Each window of destabilization shows a systematic sequence of pulse broadening with sub-structure and pulse amplitude redistribution. Sample pulses show pulse broadening with sub structure for (b) the first pulse in the cavity while the second pulse appears stable, and (c) the second pulse destabilized with the first pulse stable.

3.3 Semi-stable 4th harmonic mode-locking (HML)

The region bounded by the red line in Fig. 3 is found to correspond to semi-stable 4th HML. Figure 8 (a) shows the space-time representation of 0.5 μs at the beginning of the 250 μs time series, covering 100 round-trips. The operating point is 990 nm with 23 A pump current. The corresponding temporal trace for just over one round-trip time is shown in Fig. 8 (b), while, Figs. 8(c) and 8(d) show the same for a time which begins at the 45000th round-trip. Operating points exhibiting this dynamic have a characteristic shorter wavelength than the gain peak, medium to high pump laser diode currents, and high average output power greater than 1 W. There are four pulses in each round-trip with one pulse observed every quarter of a round-trip, ie, every ~1.28 ns. The pulses are observed to have broadened, to have sub peaks on the trailing edge, and a pulse shape which varies over time. The semi-stability in the system arises from the pulses having fixed temporal positions over the entire time series but variations are observed in their relative amplitudes and durations. The variation in pulse amplitude of any of the pulses is observed to be periodic and this is reflected in the RF

Optics EXPRESS

spectrum which shows two strong sideband spectral peaks at ~33 MHz separation from the cavity resonant frequency at ~196.15 MHz.

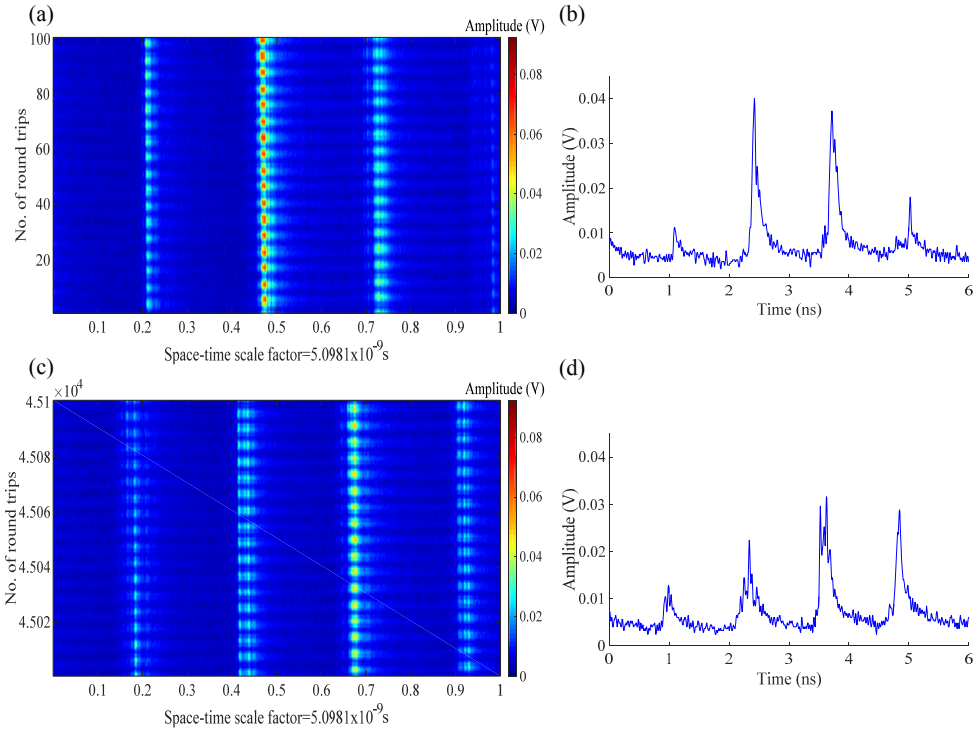

Fig. 8. (a), (c) Space-time representation over for (a) 0-0.5 μs and (c) ~229.41- 229.92 μs from the time series captured at 990 nm, 23 A. Sample temporal trace from space-time representations shown on the left respectively for (b) the 1st and (c) 45000th round-trip.

3.4 Mode-locking of few modes

A partial mode-locking regime is shown as the light blue region in Fig. 3. It exhibits high average output power of greater than 1 W, but, there is also a CW signal component to the time series with fast fluctuations in amplitude as shown in Fig. 9. Figure 10 shows the space-time representation of a 0.5 μs subset of the 250 μs time series, covering 100 round-trips. This emphasizes the constancy of the functional profile of the broad pulse component of the time trace within each round-trip over time. This dynamical behavior is observed at shorter wavelengths than the gain peak just outside the region of semi-stable 4th HML, and at higher laser diode pump currents. In the RF spectrum the component corresponding to the fundamental cavity resonant frequency has an amplitude of ~54 dB above the noise floor which is ~16 dB less than observed for FML The harmonic levels above the noise floor are observed as follows: second harmonic ~25 dB, other even harmonics between 30 and 40 dB, and higher odd harmonics ~30-45 dB. These values are between 25 and 45 dB less than the analogous peaks in the RF spectrum for FML. Overall they indicate that the mode coupling between a mode and its nearest neighbors is significantly stronger than between a mode and any mode further removed. This is consistent with the time trace which can be interpreted as close to that for three locked modes. In all cases, the RF peaks have noisy, broad pedestals indicating high timing jitter. The autocorrelation of a single round-trip from the time series shows a sharp peak at zero lag with a broad structure below. The characteristics shown by the time trace, space-time diagram, RF spectrum and the autocorrelation all indicate the initial stage of pulse formation when a few modes are being locked in phase [27].

Optics EXPRESS

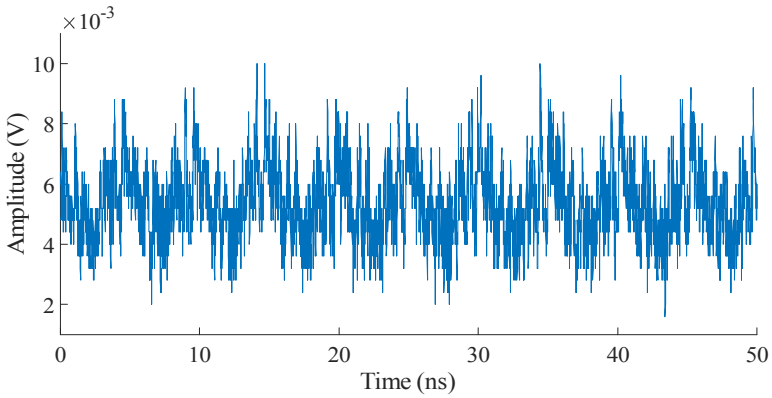

Fig. 9. 0-50 ns subset of time series captured at 986 nm and 23 A.

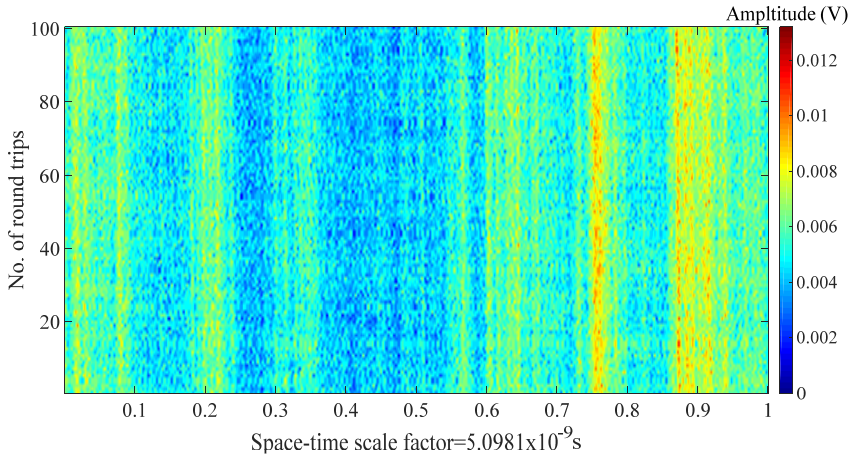

Fig. 10. 0-0.5μs subset of time series captured at 986 nm, 23 A showing dynamics over 100 round-trips of the region where the pulse formation is in the initial stages.

3.5 The CW region

The CW region is marked with a dark blue line boundary in Fig. 3. Operation in the region shows no pulsing and has a low average output power. CW behavior is exhibited at pump laser diode currents from threshold to 21 A, and for VECSEL output wavelengths above the gain peak and lying outside the FML region. The RF spectrum, obtained from a fast Fourier transform of the time series shows a small RF peak at 196.124 MHz with a magnitude of ~5 dB above the noise floor which is ~65 dB less than the RF peak at fundamental cavity resonant frequency observed for FML regime. The second harmonic RF peak has a magnitude of ~12 dB above noise floor. This is ~56.5 dB less than the strongest second harmonic cavity resonant frequency in the RF spectrum of the laser operated in the FML regime. The space-time plot for a time series from this region reflects the noise level of the time series and does not show any structure. Hence it is not shown.

4. Summary and conclusion

A detailed experimental study of the different dynamical outputs of a long-cavity (PRF ~200 MHz) VECSEL is reported. Five distinct dynamical regimes were mapped for the parameter space studied.

The fundamental passively mode-locked region, for which the system is primarily designed, is observed for a wavelength tuning range of about 5 nm. This wavelength range

Optics EXPRESS

has a longer center wavelength as the laser diode pump power is increased (992 nm at 22 A, 989 nm at 19 A). A transition to CW, low average power, operation is observed at longer wavelengths beyond the FML region. Several different types of pulsed dynamical output are observed on the short wavelength side of the FML region. Also, at shorter wavelengths and at optical pump powers below ~11.4 W the transition from FML is for lasing to cease, ie there is a higher threshold power for lasing at shorter wavelengths.

The most extensive region of non-FML output at the shorter wavelengths is a region of semi-stable 4th harmonic mode-locking, adjacent to the FML region. Average output powers which are more than 40% larger than for the same pump power in the FML region are achieved in this region. This suggests that a higher gain is being accessed in the 4th HML mode of operation. This higher gain might be able to be harnessed in FML in the future if theoretical understanding leads to modifications in system design and operation that may achieve this. A systematic sequence of the (i) amplitude variation of the 4 pulses and (ii) functional form of the 4 pulses is observed over time in semi-stable 4th HML. That the system transitions to semi-stable 4th HML is consistent with prior reports which have identified that the placement of cavity elements at distances that match a shorter cavity length associated with a desired harmonic (e.g [28]. for third harmonic ML of an Er:Yb:glass laser) can allow robust HML at that harmonic to be achieved. Here-in, the cavity length is divided into approximate quarters so robust 4th HML is not to be expected but this feature of the cavity design most likely explains the semi-stable 4th HML.

At still shorter wavelengths than the semi-stable 4th HML region there is a region of incomplete mode-locking. Here the output power in time shows a low Q modulation with the period of the round-trip time. This is indicative of locking of a small number of longitudinal modes of the cavity. The remaining types of output observed, include a single operation point (985 nm and 23 A) where stable double pulsing occurs with two pulses separated by 1.28 ns (~1/4 of the round-trip time) and ~3.81 ns (~3/4 of the round-trip time). The slight deviation in the pulse separation, observed for double pulsing, away from being an exact fractional multiple of the laser cavity round-trip time is consistent with previous work as presented in [29], where VECSELs are shown to have the ability to optimize carrier usage during multi-pulsation regimes by producing slightly temporally-shifted double pulses. A single operating point (988 nm and 21 A) shows a similar double pulsing output, but with windows of time within the time series, at a long period, of destabilization of one of the pulses at a time starting with the first pulse. The remaining mode of operation, observed at two operating points with the shortest wavelengths and mid-range pump powers (985 nm, 23 A and 986 nm, 22 A), is fundamental mode-locking with windows of the time series, at a long period, where the mode-locking is destabilized. Both destabilized sub-region of a dynamical regime show temporally systematic evolution of pulse sub-structures over hundreds of round-trips that are successfully captured by the acquisition setup. There is no shortage of candidates for physical nonlinearities that may be contributing to such destabilization including induced self-amplitude modulation as a result of detuning between resonance peaks of optical-stark and exciton absorption [30–33].

The ability to monitor long time series with high temporal resolution allows the analysis of instabilities at low frequencies. The data show the development of sub-structure within the pulse and a transient shift within round-trip time window during the instability. However, after the instability the pulses recover the old position within the round-trip time window within the resolution of the experiment.

Overall, the FML VECSEL transitions to CW operation when the operation wavelength is tuned above that of the peak of the gain. It produces a range of different pulsed dynamical outputs when the operation wavelength is tuned below that of the peak of the gain. The transitions between these different pulsed outputs are systematic and, in principle, should be able to be theoretically understood.

Optics EXPRESS

Computational models developed to-date for mode-locking analysis for VECSELs have incorporated numerous fundamental parameters accounting for the interplay between the gain of the semiconductor gain chip, group velocity dispersion, the absorption of the SESAM, and, cavity sub-resonances, resulting in characterization of the standard pulsed-regime with considerable accuracy [6,7,12,29,34,35]. Hence, it will be a future challenge for theorists in laser physics to possibly research a model that would predict the types of dynamical output that have been observed, and the systematic transitions between them. Interplay between the gain of the semiconductor gain chip and the absorption of the SESAM, and, sub-cavity resonances are all important considerations.

Funding

Macquarie University (iMQRES15, 42410984); Science and Industry Endowment Fund (SIEF) (RP-04 174); Royal Society (IE130238).

Acknowledgments

Tushar Malica is supported by an International Macquarie University Research Excellence (iMQRES) Higher Degree Research Scholarship. We are grateful for the Researcher Exchange grant from the Royal society. We are also very grateful to Tektronix Inc. and TeleDyne LeCroy Corp. for lending us the high-end oscilloscopes without which these investigations would not have been possible.